Formation of core/shell structured cobalt/carbon nanoparticles by pulsed laser ablation in toluene

H. Y. Kwong, M. H. Wong, C. W. Leung, Y. W. Wong,[a] and K. H. Wong
Department of Applied Physics, The Hong Kong Polytechnic University, Hung Hom, Kowloon, Hong Kong Special Administrative Region, People's Republic of China

Magnetic cobalt nanoparticles encapsulated in shells of layered structure have been produced by the technique of pulsed laser ablation in toluene. The morphology, microstructure, and magnetic properties of the prepared nanoparticles were characterized by electron microscopy, micro-Raman spectroscopy, and superconducting quantum interference device magnetometry, respectively. The results indicated that the cobalt nanoparticles fabricated are noncrystalline but coated with the graphitic carbon layers. It is believed that the formation of these carbon layers well-protect the cobalt nanoparticles to be oxidized thus maintaining the superparamagnetic property. This is an important feature that makes the cobalt nanoparticles a useful material for medical and many other magnetic based applications. © *2010 American Institute of Physics*. [doi:10.1063/1.3457216]

I. INTRODUCTION

Nanosized materials have attracted much attention due to their interesting properties and potential applications in various areas, such as optical and magnetic devices as well as the chemical sensors.[1] Many techniques either physical or chemical for preparing nanoparticles or nanostructured materials have been proposed, each of this method has its own advantages and suitability for certain material systems. Among these techniques pulsed laser ablation of bulk solid target either in vacuum or in gas medium to produce nanosized particles has been found to be one of the most versatile methods, because of the easy manipulation of laser beam as well as the almost unlimited applicable material systems.[2–4] Despite these advantages the broad size distribution of the particles produced and the materials oxidation during the ablation have limited the application of this technique to become a commonly practical method. However, using high power pulsed-laser with ablation process taking place in liquid (PLAL) would be an alternative and promising method. On the one hand, the produced particles can be well dispersed in liquid where the large particles will be settled and separated from the smaller particles[5] and on the other hand, oxidation of the nanoparticles could be easily controlled if the liquid selected in the operation is oxygen-free. PLAL technique was first reported by Patil *et al.*,[6] in which a metastable phase of iron oxides was synthesized by ablating an iron target in water. Subsequently, several groups demonstrated that nanosized metal particles can be produced by ablating metal targets in water or other liquids.[7–11] Size control of the nanoparticles and formation of metal compounds are also possible by changing the ablation parameters, such as the selection of liquids or adding suitable organic surfactants.[12–15]

Laser ablation in toluene has been reported for preparing carbon-coated gold nanoparticles.[16] However, not many further investigations of other materials in toluene have been reported, especially for the fabrication of magnetic nanoparticles. Intriguing potential applications of carbon-coated magnetic nanoparticle systems are emerging, such as the magnetic memory devices, drug delivery, and tumor therapy.[17–19] In this paper, we report the results on the preparation of cobalt nanoparticles using PLAL technique at room temperature, with the metal cobalt target immersed in toluene. Without the addition of surfactants, cobalt nanoparticles with graphitic carbon coating were produced. The morphology, structure, and magnetic properties of these nanoparticles will be discussed in detail in the following sections.

II. EXPERIMENTAL

Figure 1 is the schematic diagram of the PLAL setup used in this study. The metal disk of cobalt target (2.5 cm in diameter) was first polished with abrasive paper down to grit 1500, followed by ultrasonic cleaning in acetone and then ethanol. It was then mounted inside the fused silica container filled with toluene. The container was fixed on a vertically mounted computer-controlled translation stage, moving in the plane normal to the laser beam direction. Nd:YAG laser (Spectra-Physics GCR 16) of second harmonic (λ =532 nm) with 10 ns pulse duration at a repetition rate of 10 Hz was employed in the ablation process. The laser beam was focused onto the target surface to a spot diameter of about 1.2 mm, such that the laser fluence was about 20 J/cm^2. As the container moved, the focused laser beam

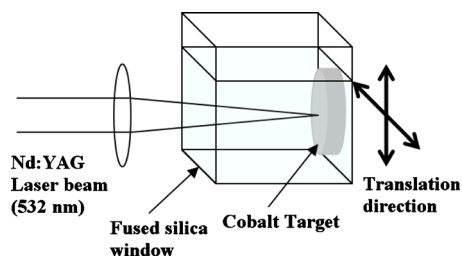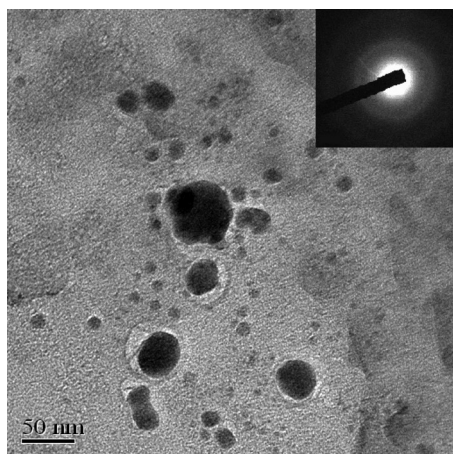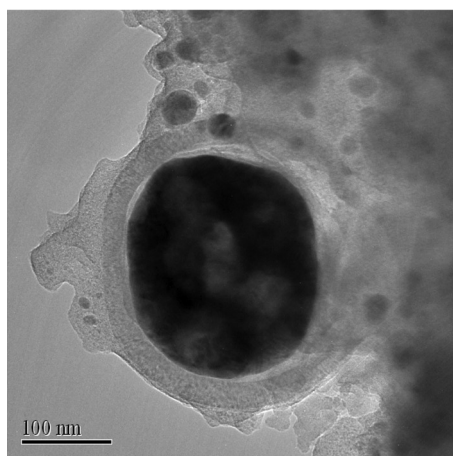

FIG. 1. (Color online) Schematic diagram of the PLAL setup.

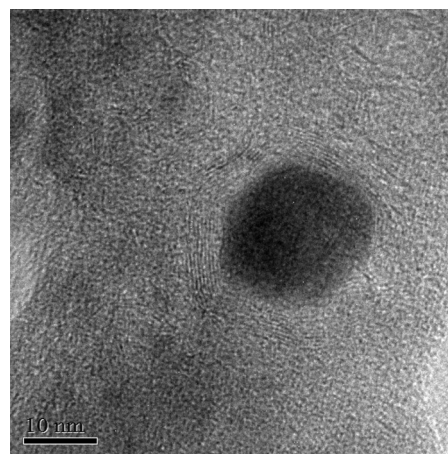a)Electronic mail: apaywwon@inet.polyu.edu.hk.

(a)

(b)

FIG. 2. (a) TEM image of the collected samples prepared by PLAL in toluene. Inset is the SAED of the image showing the noncrystalline structure of the particles obtained. (b) The core/shell structure of the nanoparticles can be seen clearly in this particularly large particle.

(a)

(b)

FIG. 3. (a) and (b) high resolution TEM images of the individual cobalt nanoparticles showing the graphitic shell structure.
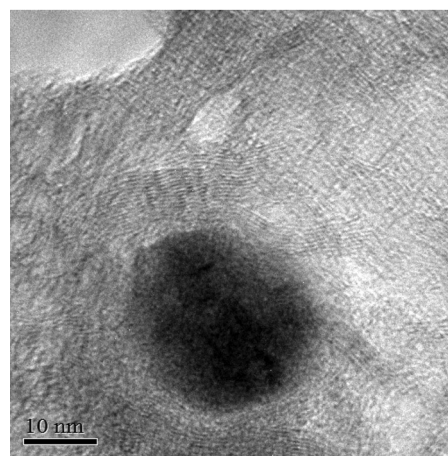
was rastering across the target surface to ensure a uniform ablation of the metal. The laser ablation time was kept at about 10 min for each collection of the colloidal solution. The ablated particles were then collected by a magnet placed adjacent to the container for 24 h. The samples obtained were subsequently characterized by the transmission electron microscope (JEOL JEM 2010) and micro-Raman spectroscope (Horiba HR800 with Olympus BX41, 488 nm laser). The magnetic properties of the samples were measured using the superconducting quantum interference device.

III. RESULTS AND DISCUSSION

Figure 2(a) is the transmission electron microscope (TEM) image of the collected sample, which shows that the range of size of the particles is about 5 to 70 nm. From the energy-dispersive X-ray spectroscopy (EDX) results provided by the TEM, the scattered particles are cobalt. In addition, the diffused ring pattern of the selected area electron diffraction (SAED) of the nanoparticles as shown in the inset of Fig. 2(a) reveals that the nanoparticles are of amorphous structure. It is believed that in each shot of laser pulse of 10 ns duration, the plasma produced in the vicinity of the target

surface quenches rapidly after the ablation where crystallization of the metal is almost suppressed, therefore, the as-prepared particles formed in such a drastic condition are noncrystalline. On the other hand, these nanosized cobalt particles show no serious agglomeration but with one interesting common feature, the larger particles exhibit an obvious core/shell structure. In order to show this feature more clearly, a larger particle was selected as shown in Fig. 2(b) of which the core/shell structure is evident and the thickness of the shell is about one-tenth of the average diameter of the particle. This feature has been found in almost all the particles collected. Since the liquid used in the PLAL is toluene, which is an aromatic liquid, the graphitization of the hydrocarbon in the high temperature plasma does happen, as a result it forms a carbon shell enclosing the cobalt nanoparticles.

In the high resolution TEM images of the nanoparticles as illustrated in Figs. 3(a) and 3(b), the layer structure of the shells are obvious. The measured layer separation is about 0.36 nm, which is close to the bulk graphite layer spacing. The overall thickness of the shell is about one quarter of the average diameter of the particles, which is larger in proportion compared with the shell thickness of the large particles as shown in Fig. 2(b). Another feature that should be noted is
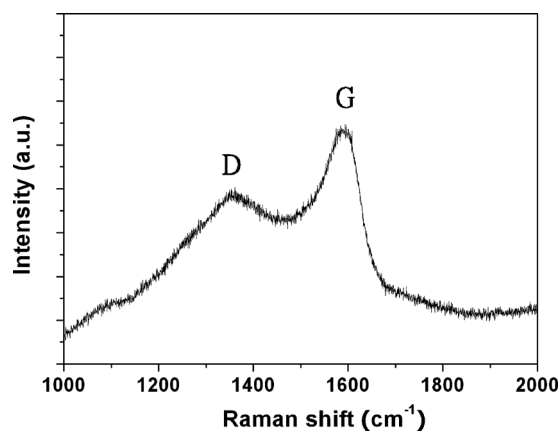
FIG. 4. Micro-Raman spectrum of the cobalt nanoparticles on glass substrate.

FIG. 5. ZFC and FC magnetization curves as a function of temperature in 50 Oe applied magnetic field from 5 to 300 K.

the closeness of the shell about the cobalt particles. As shown in Fig. 3(a), the graphitic layer almost encloses the whole cobalt particle, but in comparison with the particles shown in Fig. 3(b), the graphitization is incomplete with the intervention of amorphous carbon to enclose the cobalt nanoparticle. As a matter of fact, some core/shell nanoparticle systems, such as gold, silver, or iron oxide in graphitic shells prepared by PLAL or other methods in liquid have been reported in literatures.[16,20–22] Almost with no exception, these systems were produced in aromatic liquid like toluene or benzonitrile,[16] while those nanoparticles prepared in hexane, a linear hydrocarbon, by laser ablation did not show any graphitic shell structure.[9,11] It can be deduced that the aromatic ring structure of the liquid is an essential condition to form the graphitic shells.

The collected particles have been further studied by micro-Raman spectroscopy. As shown in Fig. 4, two broad peaks are found in the Raman spectrum that indicates the existence of the graphitic carbon in the sample. The more intense peak at around 1589 cm^{-1} (G band) is attributed to the stretching vibration in the basal-plane of the crystalline graphite, while the other peak at 1357 cm^{-1} (D band) is due to the vibration of the defects in the hexagonal basal-planes of the graphitic layers. In general, the half width of the G band of the crystalline graphite is no larger than 50 cm^{-1}, but the half width of G band shown in Fig. 4 is more than 200 cm^{-1}, it implies the graphitic layers structure of the sample has a relatively larger interlayer spacing than the graphite.[23,24] Indeed, this imperfect graphitization is evidenced also by the D band to G band integrated intensity ratio (I_D/I_G) which is about 1.8 for the collected samples, i.e., the D band vibration intensity due to the presence of disordered lattice structure[25,26] is significantly larger. Nevertheless, the result from the micro-Raman spectrum further verifies the graphitic nature of the layered shell structure, which coexists with the disordered carbon matrix where the nanoparticles are encapsulated.

The formation of the carbon/nanoparticles of core/shell structures as obtained from the PLAL process can be explained by the nucleation and growth mechanisms.[27] Immediately after the laser energy is absorbed by the cobalt target, a high temperature and pressure plasma plume of cobalt ions
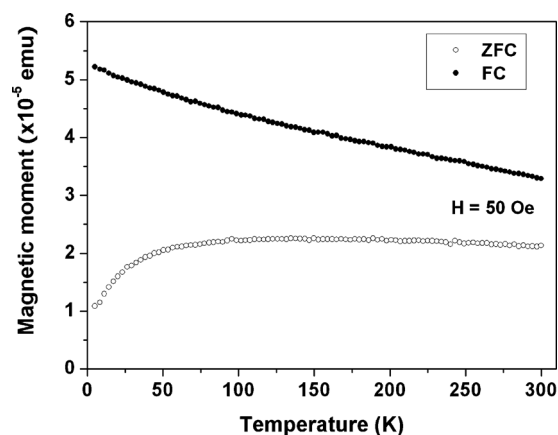
is created at the solid–liquid interface. When the temperature and pressure of the plasma plume decrease, the metal ions condense rapidly and form cobalt particles. Toluene breakdown in the vicinity of the plasma will occur simultaneously which produces the highly active carbon chains, carbon rings fragments as well as the carbon atoms,[28] the carbon chains and rings then further polymerize to form the graphitic carbon layers. The newly formed cobalt clusters once surrounded by these graphitic carbon layers, further growth of the cobalt nanoparticles is prohibited. They may continue to absorb the laser energy producing a localized heating effect. Pyrolysis of toluene can be effective and so the high temperature and carbon species favor the growth of the thin graphitic carbon layer into a thicker one surrounding the amorphous cobalt nanoparticle core. Moreover, certain amounts of carbon atoms can be "trapped" inside the cobalt core during the rapid condensation process. However, the solubility of carbon in cobalt is low[29] and the cobalt carbide is thermodynamically unstable, thus it is unlikely to form the metastable cobalt carbide in the PLAL process.

Cobalt nanoprticles are well known of their attractive magnetic properties due to the nanosize effect. They could be superparamagnetic at room temperature, but become ferromagnetic at low temperature. The effect of the graphitic shell on the magnetic behavior of the cobalt nanoparticles will be of great concern, as it will be beneficial in certain medical applications. Figure 5 shows the results of magnetizations of the sample under zero field cooling (ZFC) and field cooling (FC), respectively, as a function of temperature from 300 K to 5 K. For the ZFC curve (open circles), the samples were cooled down to 5 K in the absence of magnetic field and then the magnetization was measured at a field of 50 Oe as the sample was heated up to 300 K. The FC curve (solid circles) was measured by cooling the samples to 5 K in the presence of 50 Oe and then taking the magnetization measurement while heating up the samples to 300 K. Though the nanoparticles are with the core/shell structure, their magnetic properties can still be clearly observed. In the FC process, the magnetic moment of the sample is about 5.2×10^{-5} emu at 5 K and decreases gradually when the temperature is increased, whereas in the ZFC process, the magnetic moment of the sample is about 1.0×10^{-5} emu at 5 K, and it in-
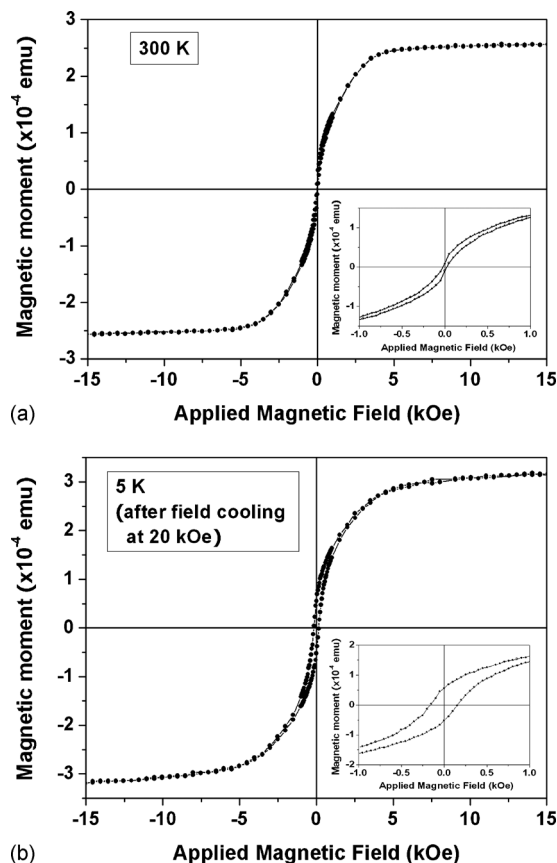
FIG. 6. Magnetization curves of the samples (a) measured at 300 K (b) measured at 5 K after cooling down the sample in the presence of 20 kOe magnetic field.

creases rapidly with temperature and reaches a maximum of 2.3×10^{-5} emu at about 130 K, then decreases slightly up to room temperature. As a matter of fact, these are common features for many ferromagnetic nanoparticle systems. The "peak" in the ZFC curve is associated with the blocking temperature of the nanoparticles at which the average relaxation time is comparable to the time scale of magnetization measurement. The large bifurcation between the ZFC and FC curves originates from the large particle-size distribution of the samples. Both curves do not merge together even at 300 K which implies that some of the particles are still in ferromagnetic state at that temperature. Indeed, particles with diameters larger than 20 nm could be found in the collected samples, which are larger than the critical diameter to be superparamagnetic.[30,31] These larger particles with remanent magnetization at room temperature lead to the observed higher magnetic moments in the FC curve. The magnetic hysteresis curve measured at 300 K is given in Fig. 6(a). The sample exhibits a very small hysteresis effect (as shown in the inset) with a coercive field just about 24 Oe, which reflects the superparamagnetic property of the sample. Figure 6(b) shows the magnetization curve of the sample measured at 5 K after cooling down in the presence of a 20 kOe magnetic field. This strong biased magnetic field is intended to apply for observing any exchange bias effect, which would occur if there is any ferromagnetic/antiferromagnetic interface. The exchange coupling or exchange bias at the interface would lead to a shift in the coercive field in the hyster-

esis loop after the sample being cooled down in the presence of a large magnetic field.[32] The results show that the coercive field (as shown in the inset) is about 162 Oe, which is significantly large compared to the room temperature coercive field. It implies that the sample is ferromagnetic at 5 K. In addition, the symmetric hysteresis loop reveals that no exchange bias effect has been occurred, i.e., no ferromagnetic/antiferromagnetic interface has been formed in the cobalt nanoparticles. As if cobalt is oxidized of which the cobalt oxide is antiferromagnetic, there will be a cobalt/cobalt oxide interface having the ferromagnetic/antiferromagnetic interaction. It is believed that the graphitic shells on the cobalt nanoparticles surface serve a good protection to avoid the cobalt nanoparticle from forming an oxide layer.

IV. CONCLUSION

Fabrication of core/shell structured carbon-coated cobalt nanoparticles was successfully demonstrated by the PLAL technique in toluene. TEM and the micro-Raman spectroscopy confirm the formation of graphitic carbon layer. The magnetic measurement, on the one hand reveals the superparamagnetic and ferromagnetic properties of the nanoparticles, on the other hand implies the nanoparticles are well protected from oxidation by the graphitic shell. This study shows that the PLAL technique is applicable in fabrication of magnetic nanoparticles protected with the graphitic shell.

[1]F. E. Kruis, H. Fissan, and A. Peled, J. Aerosol Sci. **29**, 511 (1998).
[2]Q. Li, T. Sasaki, and N. Koshizaki, Appl. Phys. A: Mater. Sci. Process. **69**, 115 (1999).
[3]Happy, S. R. Mohanty, P. Lee, T. L. Tan, S. V. Springham, A. Patran, R. V. Ramanujan, and R. S. Rawat, Appl. Surf. Sci. **252**, 2806 (2006).
[4]V. Dureuil, C. Ricolleau, M. Gandais, C. Grigis, J. P. Lacharme, and A. Naudon, J. Cryst. Growth **233**, 737 (2001).
[5]G. W. Yang, Prog. Mater. Sci. **52**, 648 (2007).
[6]P. P. Patil, D. M. Phase, S. A. Kulkarni, S. V. Ghaisas, S. K. Kulkarni, S. M. Kanetkar, S. B. Ogale, and V. G. Bhide, Phys. Rev. Lett. **58**, 238 (1987).
[7]A. V. Simakin, V. V. Voronov, G. A. Shafeev, R. Brayner, and F. Bozon-Verduraz, Chem. Phys. Lett. **348**, 182 (2001).
[8]S. I. Dolgaev, A. V. Simakin, V. V. Voronov, G. A. Shafeev, and F. Bozon-Verduraz, Appl. Surf. Sci. **186**, 546 (2002).
[9]G. X. Chen, M. H. Hong, B. Lan, Z. B. Wang, Y. F. Lu, and T. C. Chong, Appl. Surf. Sci. **228**, 169 (2004).
[10]T. Tsuji, T. Hamagami, T. Kawamura, J. Yamaki, and M. Tsuji, Appl. Surf. Sci. **243**, 214 (2005).
[11]K. Kawaguchi, J. Jaworski, Y. Ishikawa, T. Sasaki, and N. Koshizaki, J. Magn. Magn. Mater. **310**, 2369 (2007).
[12]F. Mafuné, J. Y. Kohno, Y. Takeda, and T. Kondow, J. Phys. Chem. B **104**, 9111 (2000).
[13]F. Mafuné, J. Y. Kohno, Y. Takeda, and T. Kondow, J. Phys. Chem. B **105**, 5114 (2001).
[14]C.-H. Liang, T. Sasaki, Y. Shimizu, and N. Koshizaki, Chem. Phys. Lett. **389**, 58 (2004).
[15]S. Besner, A. V. Kabashin, and M. Meunier, Appl. Phys. Lett. **89**, 233122 (2006).
[16]V. Amendola, G. A. Rizzi, S. Polizzi, and M. Meneghetti, J. Phys. Chem. B **109**, 23125 (2005).
[17]W. S. Seo, J. H. Lee, X. Sun, Y. Suzuki, D. Mann, Z. Liu, M. Terashima, P. C. Yang, M. V. McConnell, D. G. Nishimura, and H. Dai, Nature Mater.

5, 971 (2006).

[18] A. Sharma, H. Nakagawa, and K. Miura, Carbon **44**, 2089 (2006).

[19] Y. Xu, M. Mahmood, Z. Li, E. Dervishi, S. Trigwell, V. P. Zharov, N. Ali, V. Saini, A. R. Biris, D. Lupu, D. Boldor, and A. S. Biris, Nanotechnology **19**, 435102 (2008).

[20] A. H. Lu, W. C. Li, N. Matoussevitch, B. Spliethoff, H. Bonnemann, and F. Schuth, Chem. Commun. (Cambridge) **2005**, 98.

[21] C. Yu and J. S. Qiu, Chem. Eng. Res. Des. **86**, 904 (2008).

[22] Y. L. Hsin, C. F. Lin, Y. C. Liang, K. C. Hwang, J. C. Horng, J. A. A. Ho, C.-C. Lin, and J. R. Hwu, Adv. Funct. Mater. **18**, 2048 (2008).

[23] R. J. Nemanich and S. A. Solin, Phys. Rev. B **20**, 392 (1979).

[24] Y. Lu, Z. Zhu, and Z. Liu, Carbon **43**, 369 (2005).

[25] F. Tuinstra and J. L. Koenig, J. Chem. Phys. **53**, 1126 (1970).

[26] B. O. Boskovic, V. Stoljan, R. U. A. Khan, S. Haq, and S. R. P. Silva, Nature Mater. **1**, 165 (2002).

[27] R. Fabbro, J. Fournier, P. Ballard, D. Devaux, and J. Virmont, J. Appl. Phys. **68**, 775 (1990).

[28] K. Toyota, T. Tanaka, S.-I. Nishiwaki, S. Nakashima, and T. Okada, J. Photochem. Photobiol., A **141**, 9 (2001).

[29] *Binary Alloy Phase Diagrams*, 2nd ed., edited by T. B. Massalski (ASM International, Materials Park, Ohio, 1990), pp. 835–836.

[30] W. Gong, H. Li, Z. Zhao, and J. Chen, J. Appl. Phys. **69**, 5119 (1991).

[31] X. Batlle and A. Labarta, J. Phys. D: Appl. Phys. **35**, R15 (2002).

[32] J. Nogues and I. K. Schuller, J. Magn. Magn. Mater. **192**, 203 (1999).